DOI: 10.1002/cphc.200500549

Highly Anisotropic Orbitally Dependent Superexchange in Cyano-Bridged Clusters Containing Mn(III) and Mn(II) Ions

Andrew Palii,*[a] Sergey M. Ostrovsky,[a] Sophia I. Klokishner,[a] Boris. S. Tsukerblat,*[b] and Kim R. Dunbar*[c]

We study the orbitally dependent magnetic exchange in cyanide-based clusters as a source of the barrier for reversal magnetization. We consider the Mn(III)–CN–Mn(II) dimer and linear Mn(II)–NC–Mn(III)–CN–Mn(II) trimer containing octahedrally coordinated Mn(III) and Mn(II) ions with special emphasis on the magnetic manifestations of the orbital degeneracy of the Mn(III) ion. The kinetic exchange mechanism involves the electron transfer from the single occupied t_2 orbitals of the Mn(II) ion $[^6A_1\left(t_2^3e^2\right)$ ground state] to the singly occupied t_2 orbitals of the Mn(III) ion $[^3T_1\left(t_2^4\right)$ ground state] resulting in the charge-transfer $^5T_2\left(t_2^2e^2\right)_{Mn(III)}-{}^2T_2\left(t_2^5\right)_{Mn(II)}$ state of the pair. The deduced effective exchange Hamiltonian that takes into account orbital degeneracy leads to an essentially non-Heisenberg energy pattern. The energy levels are shown to be dependent on both spin and orbital quantum numbers, thus providing direct information about the magnetic anisotropy of the system. Along with the magnetic exchange, the model includes an axial component of the crystal field and spin–orbit coupling operating within the ground $^3T_1\left(t_2^4\right)$ cubic term of the Mn(III) ion. We have shown that under certain conditions both named interactions lead to the occurrence of the barrier for the reversal of magnetization, which significantly increases when passing from the dimer to the trimer. This provides a possible way for raising the magnetic barrier in the family of cyano-bridged manganese clusters.

1. Introduction

One of the most exciting developments of molecular magnetism in the last decade is the discovery of metal clusters exhibiting magnetic bistability of an entirely molecular origin, compounds that are referred to as single-molecule magnets (SMM).[1] A fascinating possibile application for SMMs is information storage at the single-molecule level and for quantum computing.

The majority of molecules exhibiting SMM behavior[1] incorporate oxide-based bridging ligands, which serve to mediate the magnetic exchange coupling between metal centers. More than a decade ago the first Mn_{12} cluster was discovered to exhibit SMM behavior and this molecules and related systems have been studied in detail since this time[2–7]. Extensive efforts have been made to raise the barrier for the reversal of magnetization by increasing the nuclearity of the systems. The development of this new field of nanochemistry led to the discovery of giant clusters such as the keprelate magnetic molecule $Mo_{72}Fe_{30}$[8] and the wreath-shaped Mn_{84} cluster[9], the largest SMM synthesized to date. Nevertheless the problem of raising the magnetic barrier reversal height remains and is attracting attention towards in-depth studies of magnetic anisotropy and to the search for systems in which new, more efficient mechanisms for magnetic anisotropy can be realized.

In the last ten years metal–cyanide compounds have attracted attention as promising candidates for new cluster types for molecular nanomagnets. The cyano-bridged SMMs that have been synthesized and characterized to date can be subdivided into two groups. The first group is exemplified by the clusters $[(Me_3tacn)_6Mn(II)Mo(III)_6(CN)_{18}]^{2+}$[10] and K[(5-Brsalen)$_2$($H_2O$)$_2$ Mn(III)$_2$Cr(III)$(CN)_6]\cdot 2H_2O$[11] containing Mn(II), Mo(III), Cr(III) and high-spin Mn(III) ions with strongly quenched orbital angular momenta in the ground states. In this case the barrier for the magnetization reversal arises from the combination of the high-spin ground *S*-state of the molecule and a sufficiently large negative zero-field splitting parameter D_S. The mechanism for barrier formation in these systems is the same as for the well-known oxo-bridged clusters and can be related to the single ion (intracenter) interactions.

The metal–cyanide clusters [Mn(III)$(CN)_6]_2$ [Mn(II) (tmphen)$_2]_3$ (tmphen = 3,4,7,8-tetramethyl-1,10-phenanthroline)[12], K[(5-

[a] *Dr. A. Palii, Dr. S. M. Ostrovsky, Prof. Dr. S. I. Klokishner*
Institute of Applied Physics, Academy of Sciences of Moldova
Academy Str. 5, MD 2028 Kishinev (Moldova)
Fax:(+3732) 738 149
E-mail: andrew.palii@uv.es

[b] *Prof. Dr. B. S. Tsukerblat*
Chemistry Department, Ben-Gurion University of the Negev
Beer-Sheva 84105 (Israel)
Fax: (+972) 8-647-2943
E-mail: tsuker@bgumail.bgu.ac.il

[c] *Prof. Dr. K. R. Dunbar*
Department of Chemistry, Texas A&M University
College Station, TX 77842-3012 (USA)
Fax: (+1) 979-845-7177
E-mail: dunbar@mail.chem.tamu.ed

Brsalen)$_2$(H$_2$O)$_2$Mn(III)$_2$Fe(III)(CN)$_6$]·2H$_2$O[11] and [(Tp)$_8$(H$_2$O)$_6$Cu(II)$_6$Fe(III)$_8$(CN)$_{24}$]$^{4+}$[13] comprise the second group. A remarkable feature of the latter type of SMM is that they contain metal ions with unquenched orbital angular momenta, namely, low-spin Mn(III)[12] and Fe(III)[11,13] ions. These systems[11–13] are drastically different in several important aspects from the classic SMMs in which all the constituent metal ions are orbitally nondegenerate. Firstly, the conventional isotropic Heisenberg–Dirac–Van Vleck Hamiltonian is inapplicable to clusters containing metal ions with unquenched orbital angular momenta and more general consideration is required. In fact, an appropriate exchange Hamiltonian under the condition of orbital degeneracy should involve not only spin operators but also orbital operators, in other words, such magnetic exchange proves to be orbitally dependent and highly anisotropic[14–17] (see also ref. [18]). Secondly, in the presence of the axial crystal field acting on the low-spin Mn(III) and Fe(III) ions, their first-order orbital angular momenta give rise to a significant single ion magnetic anisotropy. One can expect that both exchange anisotropy and single ion anisotropy contribute to the global magnetic anisotropy that is responsible for the formation of the barrier for the reversal of magnetization in SMMs containing ions with unquenched orbital angular momenta.

Our first attempts to account for the first-order single ion anisotropy in Mn(III) clusters were reported in two recent papers[19,20] in which we describe a model that accounts for the existence of a barrier for the reversal of magnetization exhibited by the [Mn(III)(CN)$_6$]$_2$[Mn(II) (tmphen)$_2$]$_3$ cluster. In this model, however, the magnetic exchange was treated as an isotropic interaction. The aim herein is to examine the magnetic anisotropy of cyanide clusters that contain transition-metal ions with unquenched orbital momenta caused by the orbitally dependent exchange interaction. Along with this issue we will discuss the conditions under which such anisotropy may result in the formation of a barrier for reversal of magnetization, which is a requisite for the SMM phenomenon. To demonstrate the effects of anisotropic exchange with utmost clarity we will inspect the magnetic anisotropy for two comparatively simple model systems, namely the dimeric cluster Mn(III)–CN–Mn(II) shown in Figure 1 a and the linear trimeric cluster Mn(II)–NC–Mn(III)–CN–Mn(II) (Figure 1 b). In these systems the Mn(III) ion is assumed to be in a strong nearly cubic crystal field produced by six carbon atoms, and hence it possesses a low-spin ground $^3T_1(t_2^4)$ state with fictitious orbital angular momentum $l = 1$. Along with the exchange anisotropy, the single ion anisotropy of the Mn(III) ion will be taken into account by including the axial crystal field operating within the $^3T_1(t_2^4)$ term. The species Mn(III)–CN–Mn(II) and Mn(II)–NC–Mn(III)–CN–Mn(II) drew our attention because of the recently demonstrated ability of cyanide chemistry to obtain molecular linear clusters with orbitally degenerate ions such as the aforementioned SMMs reported in ref. [11]. In addition such model systems can be regarded as fragments of the [Mn(III)(CN)$_6$]$_2$[Mn(II)(tmphen)$_2$]$_3$ cluster whose SMM properties have been studied during the two last years.[12,19,20]

The article is organized as follows. First (Section 2), we introduce the key concept of the effective kinetic exchange Hamiltonian between orbitally degenerate magnetic ions in a crystal field. Then (Section 3) we specify the electron-transfer pathways and symmetry of the system and in this way deduce the orbitally dependent exchange Hamiltonian for a Mn(III)–CN–Mn(II) pair. The energy pattern formed by the exchange is studied in Section 4. and the qualitative consequences of the orbital degeneracy and orbital magnetic contributions are revealed. Then the model is supplemented by introducing spin–orbit coupling (Section 5) and axial crystal field (Section 6), and these interactions are shown to be closely related to strong magnetic anisotropy and to the formation of the barrier for reversal of magnetization. In Section 7 consideration is extended to the linear Mn(II)–NC–Mn(III)–CN–Mn(II) trimer and the increase of nuclearity is demonstrated to enhance the magnetic barrier. Although the concept of strong magnetic anisotropy in degenerate exchange coupled systems has already been proposed[14–17], this concept has not been explored in the area of SMMs. This is a first attempt at the theoretical study of different factors affecting the magnetic barrier in highly symmetric cyano-bridged manganese clusters.

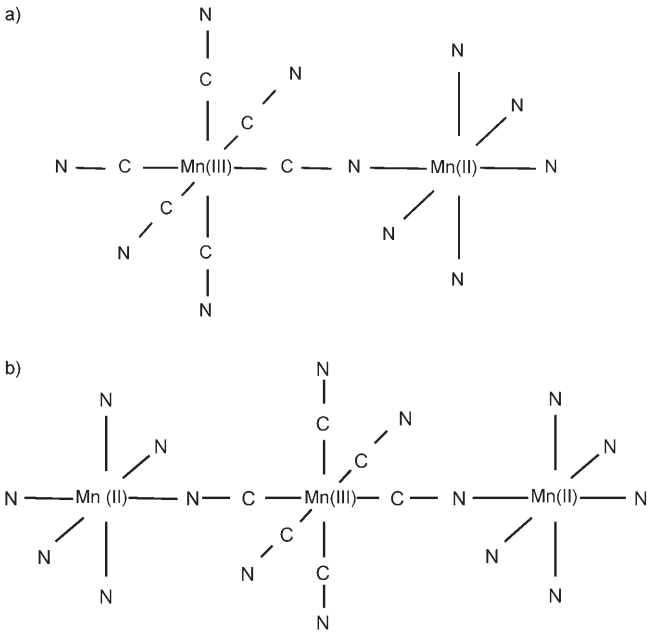

Figure 1. Structures of the model systems under consideration: a) dimer Mn(III)–CN–Mn(II), b) trimer Mn(II)–NC–Mn(III)–CN–Mn(II).

2. Hamiltonian for the Kinetic Exchange between Orbitally Degenerate Ions

Let us consider the kinetic exchange between two octahedrally coordinated transition-metal ions A and B with orbitally degenerate ground terms $^{2S_{Ag}+1}\Gamma_{Ag}(d^{n_A})$ and $^{2S_{Bg}+1}\Gamma_{Bg}(d^{n_B})$. In general, the pair is assumed to be heteronuclear so that the electronic configurations d^{n_A} and d^{n_B} are different as well as the irreducible representations Γ_{Ag}, Γ_{Bg} and full spins $S_{Ag}$and S_{Bg}. According to the basic concept of Anderson,[21] the kinetic exchange appears as a second-order contribution with respect to the intercenter electron-transfer processes so that the one-

electron transfer operator shown in Equation (1) acts as a perturbation:

$$V = \sum_{\Gamma_A\gamma_A}\sum_{\Gamma_B\gamma_B} t(\Gamma_A\gamma_A, \Gamma_B\gamma_B)\ \sum_{\sigma} C^{+}_{\Gamma_B\gamma_B\sigma} C_{\Gamma_A\gamma_A\sigma} + \text{h.c.} \qquad (1)$$

where the operator $C^{+}_{\Gamma_B\gamma_B\sigma}$ $\left(C_{\Gamma_A\gamma_A\sigma}\right)$ creates (annihilates) electron in the orbital $\varphi_{\Gamma_B\gamma_B}$ $(\varphi_{\Gamma_A\gamma_A})$ of the ion B (A) with spin projection σ, for the cubic centers Γ_A, $\Gamma_B = t_2$ or e and the symbols γ_A, γ_B label the one-electron bases, $t(\Gamma_A\gamma_A, \Gamma_B\gamma_B)$ is the corresponding hopping integral and h.c. is the complex conjugated part of *V*. Effective coupling between metal shells in cyanide clusters occurs through cyanide bridge. Within the semiempirical approach we assume a definite set of the transfer integrals (whose values incorporate the effect of the cyanobridge) and D_{4h} overall symmetry of the cluster that preserves its symmetry. We will use the real one-electron cubic basis related to the cubic local coordinate frames with the z_A (z_B) axes directed along the C_4 axis of the pair. This means that γ_A and γ_B will run over $\xi \propto yz$, $\eta \propto xz$, $\zeta \propto xy$ (t_2 basis) and $u \propto 3z^2 - r^2$, $v \propto \sqrt{3}(x^2 - y^2)$ (e basis). The operator, Equation (1), connects the ground state of the pair with the excited charge-transfer (CT) states arising from the electronic configurations $d^{n_A\mp1} - d^{n_B\pm1}$ in which one electron is transferred from the site A(B) to the site B(A).

Below we apply this general approach to the problem of the magnetic exchange between orbitally degenerate ions developed in our recent articles[14–16] in which the effective Hamiltonian of the exchange interaction is derived and its use is illustrated in detail. Application of this approach leads to the following expression for the kinetic exchange Hamiltonian operating within the ground ${}^{2s_{Ag}+1}\Gamma_{Ag}(d^{n_A})\otimes{}^{2s_{Bg}+1}\Gamma_{Bg}(d^{n_B})$ manifold of the pair:

$$\begin{aligned} H_{ex}(A,B) = &-2\sum_{\Gamma_A\Gamma_B}\sum_{\gamma_A\gamma_B\,\gamma'_A\gamma'_B} t(\Gamma_A\gamma_A, \Gamma_B\gamma_B)\ t(\Gamma_B\gamma'_B, \Gamma_A\gamma'_A) \\ &\times \sum_{\Gamma\gamma}\sum_{\Gamma'\gamma'} \langle\Gamma\gamma|\Gamma_A\gamma_A\Gamma_A\gamma'_A\rangle\ \langle\Gamma'\gamma'\mid\Gamma_B\gamma_B\Gamma_B\gamma'_B\rangle\ O^{A}_{\Gamma\gamma}\ O^{B}_{\Gamma'\gamma'} \\ &\times \left[F^{(0)}_{\Gamma\Gamma'}(\Gamma_A,\Gamma_B) + F^{(1)}_{\Gamma\Gamma'}(\Gamma_A,\Gamma_B)\ \mathbf{s}_A\mathbf{s}_B\right] \end{aligned} \qquad (2)$$

In Equation (2), $\mathbf{s}_A$ and $\mathbf{s}_B$ are the single ion spin operators, while $O^{A}_{\Gamma\gamma}$ and $O^{B}_{\Gamma'\gamma'}$ are the cubic irreducible tensor operators (matrices) acting within the orbital manifolds Γ_{Ag} and Γ_{Bg}, $\langle\Gamma\gamma|\Gamma_A\gamma_A\Gamma_A\gamma'_A\rangle$ are the Clebsch–Gordan coefficients for the O_h group. The operators $O^{i}_{\Gamma\gamma}$ are defined in such a way that their reduced matrix elements $\langle\Gamma_{ig}||\mathbf{O}^{i}_{\Gamma}||\Gamma_{ig}\rangle = (\Gamma_{ig})^{1/2}$, where (Γ_{ig}) is the dimension of Γ_{ig}, so the matrix elements of these operators coincide with the Clebsch–Gordan coefficients according to the Wigner–Eckart theorem,[22] $\langle\Gamma_{Ag}\gamma'_{Ag}|\mathbf{O}^{A}_{\Gamma\gamma}|\Gamma_{Ag}\gamma_{Ag}\rangle = \langle\Gamma_{Ag}\gamma'_{Ag}|\Gamma_{Ag}\gamma_{Ag}\Gamma\gamma\rangle$. Finally, the parameters $F^{(0)}_{\Gamma\Gamma'}$ and $F^{(1)}_{\Gamma\Gamma'}$ are expressed in terms of the energies of the CT states. The explicit expressions for these parameters are given in ref. [15].

3. Exchange Model for a Mn(III)–CN–Mn(II) Pair

In this section we describe the application of the above described formalism to the cyano-bridged Mn(III)–CN–Mn(II) pair in which the Mn(III) ion is surrounded by six carbon atoms and the Mn(II) ion is surrounded by six nitrogen atoms. We shall take into account the most important cubic component of the crystal field, therefore in the first step we assume that both metal ions are in perfect octahedral ligand fields. The ground-state term of the Mn(III) ion in strong cubic field produced by the carbon atoms is expected to be the low-spin orbital triplet ${}^3T_1(t_2{}^4)$. In contrast, the weak crystal field induced by the nitrogen atoms in cyano-bridged compounds gives rise to a ground high-spin orbital singlet ${}^6A_1\left(t_2^3e^2\right)$ for the Mn(II) ion. so the ground state of the bi-octahedral corner-shared dimer (with overall D_{4h} symmetry) will be ${}^6A_1\left(t_2^3e^2\right)_{Mn(II)} - {}^3T_1\left(t_2^4\right)_{Mn(III)}$.

To apply the general formula for the exchange Hamiltonian, Equation (2), to the Mn(III)–Mn(II) pair we will assign the indices *A* and *B* to the Mn(II) and Mn(III) ions, respectively, so that $S_{Ag}\,\Gamma_{Ag} = {}^6A_1\left[t_2^3({}^4A_2)\ e^2({}^3A_2)\right] \equiv {}^6A_1\left(t_2^3e^2\right)$ and $S_{Bg}\,\Gamma_{Bg} \equiv {}^3T_1\left(t_2^4\right)$. Since the transfer of the electron from the Mn(III) ion to Mn(II) leads to CT states with very high excitation energies we will neglect such processes and consider only the Mn(II)–Mn(III) ($A \rightarrow B$) electron transfer. The exchange pathways are now specified. There are two possible paths for the $A \rightarrow B$ electron transfer, namely, the transfer from the single occupied t_2 orbitals of the Mn(II) ion to the single occupied t_2 orbitals of the Mn(III) ion through the bonding π and antibonding π^* orbitals of the cyanide ion, and the transfer from the single occupied e orbitals of Mn(II) to the empty e orbitals of Mn(III) through the σ orbitals of the cyanide bridge (the hopping parameters corresponding to the $t_2 \rightarrow e$ transfer are expected to be negligible due to the orthogonality of the t_2 and e orbitals). At the same time recent density functional theory calculations of the exchange parameters in cyano-bridged species[23] demonstrated that the interaction through the cyanide σ orbitals is significantly smaller than the interaction through the π and π^* orbitals[24] (see also references therein). This is why only $t_2^A \rightarrow t_2^B$ transfer processes are assumed to be important and will be taken into account in our kinetic exchange model. Due to the symmetry of the system, there are two equivalent hopping parameters $t_{\xi\xi} = t_{\eta\eta} \equiv t$ associated with $\xi - \xi$ and $\eta - \eta$ overlap integrals between the t_2 orbitals of the Mn(II) and Mn(III) ions through the π and π^* orbitals of the cyanide bridge (Figure 2). At the same time the transfer integral $t_{\zeta\zeta}$ can be omitted because there is no effective overlap between the ζ orbitals (as the missing cyanide orbitals have δ symmetry). Note that the $t_2^A \rightarrow t_2^B$ transfer does not affect the e^2 subshell of the ion A (the ${}^3A_2(e^2)$ state). At the same time this transfer decreases the spin of ion A by 1/2. As a result of the electron transfer, the oxidized configuration $t_2^2e^2$ of ion A forms the term ${}^5T_2\left[t_2^2({}^3T_1)\,e^2({}^3A_2)\right] \equiv {}^5T_2\left(t_2^2e^2\right)$, which is the only ${}^5T_2$ term in d^4(Figure 3). The low-lying level of the reduced t_2^5 configuration of ion B is ${}^2T_2\left(t_2^5\right)$. We shall not take into account Coulomb mixing of this term with the excited ${}^2T_2\left(t_2^{5-k}e^k\right)$ terms.[22] We will thus assume that the $t_2^A \rightarrow t_2^B$ transfer results in the only CT

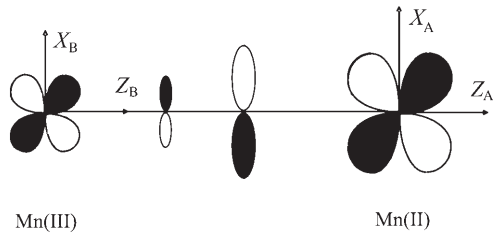

Figure 2. Scheme of overlap between t_2 orbitals of Mn(III) and Mn(II) through the π orbitals of the cyanide bridge.

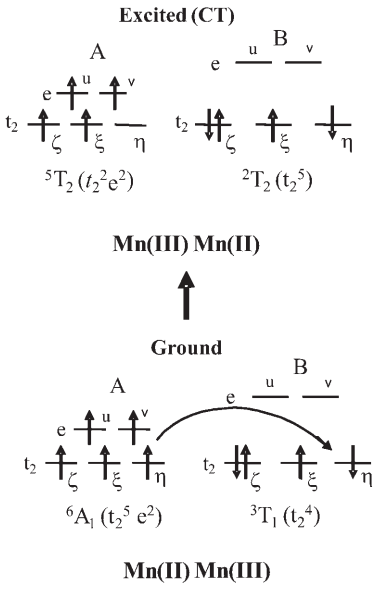

Figure 3. Scheme of the kinetic exchange mechanism for the Mn(III)–CN–Mn(II) pair.

state $^5T_2\left(t_2^2e^2\right)_A - ^2T_2\left(t_2^5\right)_B$. Within this approximation the single ion states involved in this CT state are the "pure" states, each resulting from the only electronic configuration.

The orbital schemes for the $[Mn(II)]_A[Mn(III)]_B$ pair (ground state) and $[Mn(III)]_A[Mn(II)]_B$ pair (CT state) along with the electron-transfer process connecting these states are shown in Figure 3. It is to be noted that each orbital scheme depicts only one Slater determinant (microstate) of the many-electron open-shell wave function. For example, the only determinant $\left|\xi\,\overline{\eta}\,\zeta\,\overline{\xi}\right|$ involved in the two-determinant wave function $\left|^3T_1\left(t_2^4\right),\gamma,m_s=0\right\rangle = \left(1/\sqrt{2}\right)\left(\left|\overline{\xi}\,\eta\,\zeta\,\overline{\zeta}\right| + \left|\xi\,\overline{\eta}\,\zeta\,\overline{\zeta}\right|\right)$ of the low-spin Mn(III) ion is shown in Figure 3. On the contrary, the half-filled shell $t_2^3e^2$ is represented by the only microstate $\left|^6A_2\left(t_2^3e^2\right),\ m_s=5/2\right\rangle = \left|\xi\,\eta\,\zeta\,u\,v\right|$ so the corresponding orbital scheme in this case shows the full wave function of the high-spin Mn(II) ion. The jumping electron does not change its spin projection and selects the initial and final microstates as exemplified in Figure 3.

At this point it is straightforward to adapt the general expression for the kinetic exchange Hamiltonian, Equation (2), to the Mn(III)—CN–Mn(II) pair under consideration. First we exploit the overall symmetry of the system by substituting the relevant values of the transfer integrals and Clebsch–Gordan coefficients into Equation (2). Since only spin operators act within the orbitally nondegenerate ground state of the Mn(II) ion, the orbital operators act only within the basis of the orbital triplet of Mn(III) (ion B), which leads to Equation (3):

$$H_{ex}(A,B) = -\frac{4}{3}\,t^2\left[F^{(0)}_{A_1A_1}(t_2,t_2)\,O^B_{A_1} + \left(1/\sqrt{2}\right)F^{(0)}_{A_1E}(t_2,t_2)\,O^B_{Eu}\right] - \frac{4}{3}\,t^2\left[F^{(1)}_{A_1A_1}(t_2,t_2)\,O^B_{A_1} + \left(1/\sqrt{2}\right)F^{(1)}_{A_1E}(t_2,t_2)\,O^B_{Eu}\right]\ \mathbf{s}_A\mathbf{s}_B \tag{3}$$

The orbital operators $O^B_{A_1}$ and O^A_{Eu} are represented by the matrices shown in Equation (4) in the cubic T_1 basis defined in a standard manner $\alpha \propto L_x$, $\beta \propto L_y$, $\gamma \propto L_z$:

$$O^B_{A_1} = \begin{pmatrix} 1 & 0 & 0 \\ 0 & 1 & 0 \\ 0 & 0 & 1 \end{pmatrix} \quad , \qquad O^B_{Eu} = \begin{pmatrix} -\frac{1}{2} & 0 & 0 \\ 0 & -\frac{1}{2} & 0 \\ 0 & 0 & 1 \end{pmatrix} \tag{4}$$

The parameters $F^{(k)}_{\Gamma\Gamma'}$ in Equation (3) can be found with the aid of an existing approach,[14–16] therefore we have omitted the details of the calculation and give only the final result in Equation (5):

$$F^{(0)}_{A_1A_1}(t_2,t_2) = \frac{1}{2\ \varepsilon_{A\to B}}\ , \quad F^{(1)}_{A_1A_1}(t_2,t_2) = -\frac{1}{5\ \varepsilon_{A\to B}}$$
$$F^{(0)}_{A_1E}(t_2,t_2) = -\frac{1}{2\sqrt{2}\ \varepsilon_{A\to B}},\ F^{(1)}_{A_1E}(t_2,t_2) = \frac{1}{5\sqrt{2}\ \varepsilon_{A\to B}} \tag{5}$$

where $\varepsilon_{A\to B}$ is the energy of the $^6A_1\left(t_2^3e^2\right)_A - ^3T_1\left(t_2^4\right)_B \to ^5T_2\left(t_2^2e^2\right)_A - ^2T_2\left(t_2^5\right)_B$ excitation.

The T–P isomorphism makes it possible to consider the ground $^3T_1\left(t_2^4\right)$ term of the Mn(III) ion (ion B) as a state possessing fictitious orbital angular momentum.[21] This allows one to express the cubic irreducible tensor O^B_{Eu} in Equation (3) in terms of the orbital angular momentum operator l_{ZB} acting within the $|l_B = 1,\ \ m_{lB} = 0,\ \pm1\rangle$ basis (where m_{lB} is the projection of the fictitious orbital angular momentum) as shown in Equation (6):

$$O^B_{Eu} = 1 - (3/2)\,l^2_{ZB} \tag{6}$$

By substituting Equation (5) and (6) into Equation (3) we arrive at the final Equation (7) for the kinetic exchange Hamiltonian of the Mn(III)–CN–Mn(II) pair:

$$H_{ex}(A,B) = -(1/2)\ J_{ex}\left(-5 + 2\ \mathbf{s}_A\mathbf{s}_B\right)\left(2 + 3\ l^2_{ZB}\right) \tag{7}$$

where the kinetic exchange parameter is given by Equation (8)

$$J_{ex} = -\frac{t^2}{15\ \varepsilon_{A\to B}} \tag{8}$$

The Hamiltonian, Equation (7), [as well as the general one in Eq. (3)] involves three types of terms: 1) the isotropic part of the exchange interaction, which has the standard form,

$-2J_{ex}\mathbf{s}_A\mathbf{s}_B$; 2) the orbital part $(15/2)\,J_{ex}l_{zB}^2$, which is independent of the spin variables and acts within the orbital space of the Mn(III) ion; 3) the mixed term $-3\,J_{ex}\mathbf{s}_A\mathbf{s}_B\,l_{zB}^2$, which is composed of spin and orbital operators; and 4) the constant term $5J_{ex}$ that results in the common shift of the energy pattern and for this reason can be omitted. The second and the third contributions are magnetically anisotropic. This anisotropy of the exchange is created by the presence of the orbital angular momentum of the orbitally degenerate Mn(III) ion and the easy axis is directed along the Mn(II)–Mn(III) axis (the *z* axis of the pair). The isotropic and anisotropic contributions to the exchange are governed by the only parameter J_{ex} so that they are of the same order and in this sense the anisotropy is strong. Such strong magnetic anisotropy was shown to be an inherent feature of the orbitally dependent exchange.[14–17] Although the Hamiltonian in Equation (7) factorizes into spin and orbital terms, the Lande rule is not valid for the whole energy pattern. In fact, the only scalar spin–spin contribution gives rise to a superimposed Lande-type pattern, with the remaining levels depending on both spin and orbital quantum numbers.

4. Energy Pattern Formed by the Magnetic Exchange in a Mn(III)–CN–Mn(II) Pair

The Hamiltonian, Equation (7), proves to be isotropic in the spin subspace and axially symmetric in the orbital subspace, so that S, M_S (the total spin of the pair and its projection) and m_{lB} are good quantum numbers. The eigenvalues of $H_{ex}(A, B)$ are calculated according to Equation (9):

$$E(S,\ m_{lB}=0) = -J_{ex}\ [-63/4 + S(S+1)]\,,$$
$$E(S,\ |m_{lB}|=1) = -(5/2)\,J_{ex}\ [-63/4 + S(S+1)] \qquad (9)$$

The energy pattern of the Mn(III)–CN–Mn(II) pair consists of two superimposed groups of energy levels with $m_{lB}=0$ and $|m_{lB}|=1$ (see Figure 4). The total spin S of the pair takes the values $S = 3/2,\ 5/2,\ 7/2$, and the energy levels within each group obey the Lande rule. The exchange splitting of both $m_{lB}=0$ and the $|m_{lB}|=1$ multiplet proves to be antiferromagnetic $(S_{gr}=3/2)$. The conclusion about the antiferromagnetic exchange splitting in each group of the energy levels is in agreement with the underlying ideas of Anderson[21] and Goodenough and Kanamori ([25] and references therein). In fact, these authors indicated that electron hopping between the half-occupied orbitals should result in the antiferromagnetic exchange coupling.

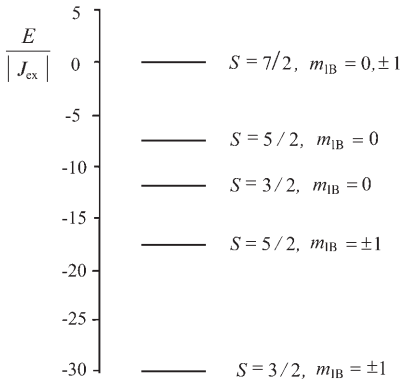

Figure 4. Energy pattern formed by the orbitally dependent magnetic exchange for the Mn(III)–CN–Mn(II) pair.

It is to be underscored that Lande's rule is not valid for the whole energy pattern; in particular, non-monotonic alternation of the levels with $S = 3/2$ and $S = 5/2$ takes place. Another important result is that the energy levels depend not only on the total spin quantum number S but also on $|m_{lB}|$. This leads to the anisotropic magnetic behavior of the system. In the magnetic field applied along the C_4 axis of the bi-octahedron the orbital contribution to the Zeeman splitting of the ground level is significant (first-order effect) because the operator $-\kappa\beta l_{zB}H_z$ possesses the following non-vanishing matrix elements within the ground level:

$$\langle S=3/2,\ M_S,\ m_{lB}=\pm1|\,-\kappa\beta l_{zB}H_z\,|S=3/2,\ M_S,\ m_{lB}=\pm1\rangle = \pm\kappa\beta H \qquad (10)$$

In Equation (10) κ is the orbital reduction factor, and the minus sign in the Zeeman operator appears due to the fact that the matrix elements of $\mathbf{l}_B$ within the T_1 and P bases are of opposite signs.[21] In contrast, the orbital contribution to the Zeeman splitting of the ground level in a perpendicular field is much smaller because it appears as a second-order effect due to the mixing of the ground level with the second excited level $(S = 3/2,\ m_{lB}=0)$ by the operator $-\kappa\beta\,(l_{xB}H_x + l_{yB}H_y)$ (Van Vleck paramagnetism). Therefore, in contrast to the Heisenberg magnetic exchange, the orbitally dependent exchange interaction described by the Hamiltonian, Equation (7), produces a strong magnetic anisotropy of the pair.

5. Influence of the Spin–Orbit Coupling and Magnetic Barrier

The spin–orbit (SO) interaction for the Mn(III) ion is stronger than the exchange coupling in the cyano-bridged Mn(II)–Mn(III) pair. Therefore, to make the analysis more realistic, we will also include in the model the SO coupling operating within the $^3T_1$ term of the Mn(III) ion. The SO coupling operator is given by Equation (11)

$$H_{SO} = -\kappa\lambda\ \mathbf{s}_B\,\mathbf{l}_B \qquad (11)$$

where $\lambda \approx -180\ cm^{-1}$ is the many-electron SO coupling parameter for the $^3T_1(t_2^4)$ term.[26] Figure 5 displays the combined effect of the orbitally dependent exchange and the SO coupling on the energy pattern of the Mn(III)–CN–Mn(II) pair. One can see that, providing $J_{ex}=0$, the energy pattern consists of three levels: $-2\kappa|\lambda|$, $-\kappa|\lambda|$ and $\kappa|\lambda|$, which correspond to the full angular momentum of Mn(III) ion $j_B = 0,\ 1$ and 2, respectively.

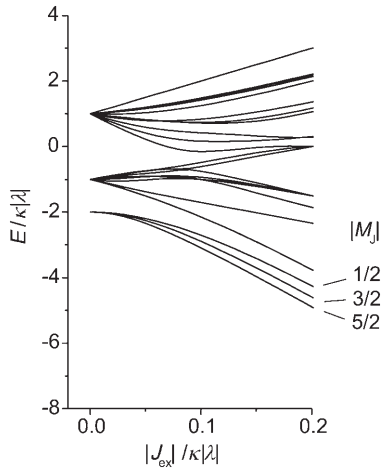

Figure 5. Combined effect of the exchange and the SO coupling on the energy levels of the Mn(III)–CN–Mn(II) pair

When the exchange interaction is switched on ($J_{ex} \neq 0$), the energies become dependent on $|M_J|$, where $M_J = m_{sA} + m_{sB} + m_{lB}$ is the projection of the total angular momentum ($m_{sA}$and m_{sB} are the spin projectionsof ions A and B). Three low-lying levels with $M_J = \pm 5/2$, $M_J = \pm 3/2$ and $M_J = \pm 1/2$ (originating from $j_B = 0$) are well isolated from the excited states and their energies monotonically increase with decreasing $|M_J|$. We thus arrive at the conclusion that the orbitally dependent exchange between the Mn(III) and Mn(II) ions in combination with the SO coupling acting within the ground state of the Mn(III) ion results in the formation of a barrier for the reversal of magnetization. The magnitude $U = E(|M_J| = 1/2) - E(|M_J| = 5/2)$ can be conventionally associated with the height of the barrier. The next level (originating from $j_B = 1$, see Figure 5) also belongs to this group of well-isolated levels but the gap between this level and the three low-lying levels (originating from $j_B = 0$) is significantly larger. One can conclude that, within the model employed, the barrier monotonically increases with increasing exchange interaction. The fourth excited level belongs to $M_J = \pm 1/2$ so it does not affect the conclusion regarding the barrier (although in the full analysis of the dymamic properties of the system this level should be taken into account).

6. Combined Effect of Single Ion and Exchange Anisotropies

The above consideration relates to the high-symmetry case when the Mn(III) ion is in the perfect octahedral surroundings of carbon atoms. In this case no local (single ion) anisotropy can appear and the orbitally dependent superexchange represents the only source of the global magnetic anisotropy of the system. Now we will focus on the case when the carbon octahedron is axially distorted along the $C_4(z)$ axis or the ions of the next coordination spheres produce a relatively weak axial crystal field. The corresponding axial crystal field term in the Hamiltonian can be presented as in Equation (12):

$$H_{ax} = \Delta\left(l_{ZB}^2 - 2/3\right) \qquad (12)$$

where Δ is the parameter of the axial field. This interaction splits the ground $^3T_1$ term of the Mn(III) ion into the orbital doublet ^3E (orbital basis $m_{lB} = \pm 1$) and the orbital singlet $^3B_2$ ($m_{lB} = 0$) in such a way that the orbital singlet (orbital doublet) becomes the ground state providing $\Delta > 0$ ($\Delta < 0$).

In previous papers[19,20] we have demonstrated that the combined action of the SO coupling and the negative axial crystal field ($\Delta < 0$) gives rise to the formation of a barrier for the reversal of magnetization even in the case when the magnetic exchange between the Mn(III) and Mn(II) ions is considered to be isotropic. In this case the exchange anisotropy is excluded and only the single ion anisotropy contributes to the global magnetic anisotropy of the cluster.

In a further development of this topic, we will examine a more general case when both types of magnetic anisotropy (local and exchange) contribute to the barrier U for the reversal of magnetization. In this consideration, it is instructive to compare two models. Model I includes isotropic exchange between the Mn(III) and Mn(II) ions described by the Heisenberg–Dirac–Van-Vleck spin Hamiltonian $H_{ex}(A, B) = -2J_{ex}\,\mathbf{s}_A\mathbf{s}_B$ with $J_{ex} < 0$ (antiferromagnetic) as well as the tetragonal component of the crystal field, Equation (12), and the SO coupling, Equation (11). Model II deals with anisotropic orbitally dependent exchange, that is, along with all named interactions; model II also includes the orbitally dependent part of the exchange Hamiltonian, Equation (7), described by the term $-(3/2)J_{ex}(-5 + 2\,\mathbf{s}_A\mathbf{s}_B)\,l_{ZB}^2$.

Figure 6 shows the value of U thus far defined as a function of the axial crystal field parameter Δ. One can see that, in the high-symmetry limit ($\Delta = 0$), the barrier disappears ($U = 0$) in the isotropic model I while, within the anisotropic exchange model II, the barrier remains non-vanishing even in the absence of local anisotropy ($\Delta = 0$). In the latter case the barrier is produced solely by the exchange anisotropy. Providing $\Delta < 0$ we obtain a non-vanishing barrier in both models, but in model II this barrier is higher. It is seen that the magnitude of the barrier monotonically increases with increasing negative axial field and saturates in the axial limit, $|\Delta| \gg |\lambda|$. A similar effect of increasing barrier with increasing axial component of

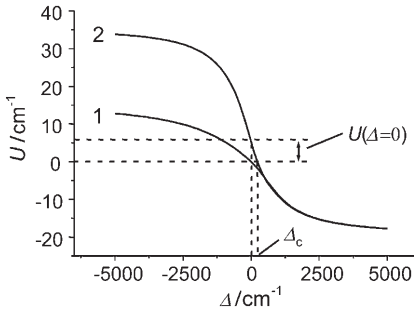

Figure 6. Dependence of the barrier for the reversal of magnetization on the axial crystal field parameter calculated for the Mn(III)–Mn(II) dimer at $\lambda = -180\ cm^{-1}$, $\kappa = 1$ and $J_{ex} = -4\ cm^{-1}$. Curve 1: isotropic exchange model (I); curve 2: anisotropic exchange model (II).

the negative crystal field was mentioned in our recent studies of the pentanuclear $Mn(III)_2Mn(II)_3$system.[20] This effect is caused by the unquenched first-order orbital magnetic contribution to the orbital doublet ^3E stabilized by a strong negative axial field. It should be emphasized that contributions to the height of the barrier arising from the single ion anisotropy and the exchange anisotropy are not additive. As can be seen from Figure 6 the exchange anisotropy enhances the effect of the axial field so that the combined effect of single ion and exchange anisotropies on the barrier is larger than that produced by the sum of the two independent contributions. This shows that the negative axial field in conjunction with the orbitally dependent superexchange provides a favorable condition for an increase in the barrier for cyanide-bridged clusters containing the low-spin Mn(III) ion.

A positive axial field stabilizes the orbital singlet $^3B_2$ in the Mn(III) ion so that, in the strong field limit, the anisotropic part of the orbitally dependent exchange disappears and the system can be described by the isotropic exchange model. At the same time, the local anisotropy also vanishes due to a reduction of the orbital angular momentum in the ground state. When the axial field reaches a critical value ($\Delta_c \approx 230$ cm^{-1} for the adopted set of parameters) the exchange anisotropy and the local one are cancelled such that, in model II, the barrier U vanishes. A further increase of Δ leads to the full suppression of the exchange anisotropy, and curves 1 and 2 merge (Figure 6).

7. Linear Trimeric Mn(II)–NC–Mn(III)–CN–Mn(II) Cluster

Now let us consider how an increase in the nuclearity affects the anisotropy of a system containing an orbitally degenerate ion. We shall study the simplest system that can be obtained by adding one cyanide unit containing the orbitally nondegenerate ion Mn(II) to the Mn(II)–NC–Mn(III) dimer. Such a linear trimeric cluster Mn(II)–NC–Mn(III)–CN–Mn(II) is depicted in Figure 1b. The two Mn(II) ions are labeled A and C, and the Mn(III) ion is donated by the letter B. The Hamiltonian of the orbitally dependent exchange, Equation (7), contains pairwise interactions and therefore can be simply extended to the case of the trimer as shown in Equation (13):

$$\begin{aligned} H_{ex} &= H_{ex}(A, B) + H_{ex}(B, C) \\ &= -(1/2)\, J_{ex}\, [-10 + 2\, (\mathbf{s}_A\mathbf{s}_B + \mathbf{s}_B\mathbf{s}_C)]\, \left(2 + 3\, l_{ZB}^2\right) \end{aligned} \quad (13)$$

Since sites A and C are equivalent, the condition $\varepsilon_{A\rightarrow B} = \varepsilon_{C\rightarrow B}$ is used while deriving Equation (13). The eigenvalues of the Hamiltonian, Equation (13), can be easily expressed, as shown in Equation (14), through the full spin of the trimer S, intermediate spin S_{AC} and quantum number m_{lB}:

$$\begin{aligned} &E(S, m_{lB}) = -(1/2)\, J_{ex} \\ &\cdot\, [-10 + S(S+1) - S_{AC}(S_{AC}+1) - s_B(s_B+1)]\left(2 + 3\, m_{lB}^2\right) \end{aligned} \quad (14)$$

The energy patterns consist of two interpenetrating Heisenberg schemes (with two different exchange parameters) for a linear trimer corresponding to $m_{lB} = 0$ and $m_{lB} = \pm 1$. As in the case of the dimer, the full Hamiltonian of the trimeric cluster also includes the operators of the SO interaction, Equation (11), and axial crystal field, Equation (12). The energy levels obtained by diagonalizing the full Hamiltonian matrix prove to be dependent on $|M_J|$, where $M_J = m_{sA} + m_{sB} + m_{sC} + m_{lB}$ is the projection of the total angular momentum of the trimer. Inspecting the low-lying part of the energy pattern calculated in this manner, one arrives at the conclusion that it can be associated with the magnetic barrier. Figure 7 shows the

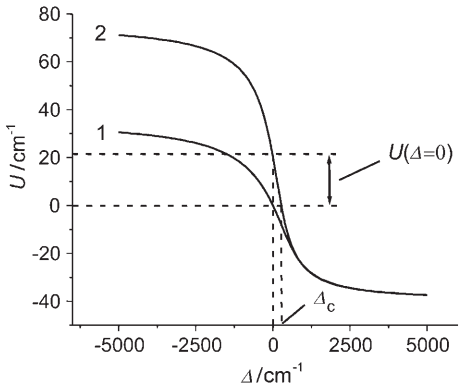

Figure 7. Dependence of the barrier for the reversal of magnetization on the axial crystal field parameter calculated for a Mn(II)–Mn(III)–Mn(II) trimer for $\lambda = -180$ cm^{-1}, $\kappa = 1$ and $J_{ex} = -4$ cm^{-1}. Curve 1: isotropic exchange model (I), curve 2: anisotropic exchange model (II).

dependence of the magnitude U of the barrier ($U = E(M_J = 0) - E(|M_J| = 5)$) on the parameter Δ calculated within the isotropic and anisotropic exchange models for the same values of the parameters as in the case of the dimer. From the comparison of Figrres 7 and 6 it follows that, for the trimeric cluster, all the trends described for the dimers are also operative, but the barrier for the reversal of magnetization for the trimer is much larger than that calculated for the binuclear cluster. For example, the value $U(\Delta = 0)$ calculated for the trimer in the framework of the anisotropic exchange model (curve 2 in Figure 7) is four times larger than the analogous value for the dimer (see Figure 6). One can also see (compare Figures 6 and 7) that the values of U obtained for the trimer in the axial limit (strong negative axial field) within the two models are at least two times larger than the corresponding values calculated for the binuclear cluster. The critical value of the axial field (Δ_c) for the trimer is $\approx$270cm^{-1}, that is, it is also larger than the value for Δ_c calculated for the dimer with the same set of parameters. This means that in the case of the trimer a stronger positive axial field is required to fully destroy the barrier created by the orbitally dependent superexchange.

An additional illustration of the enhance of the barrier with increasing nuclearity is provided in Figures 8 and 9 in which the energy levels calculated within the anisotropic exchange model are depicted for the dimer and trimer on one scale for the same set of parameters (only the low-lying levels forming the barriers are displayed). Figure 8 relates to the high-symme-

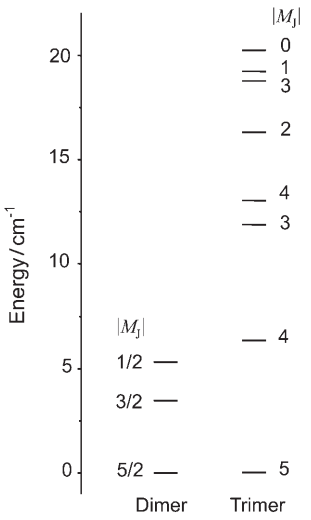

Figure 8. Comparison of the barriers for the reversal of magnetization for Mn(III)–Mn(II) (left) and Mn(II)–Mn(III)–Mn(II) (right) clusters calculated within the anisotropic exchange model with $J_{ex} = -4$ cm^{-1}, $\lambda = -180$ cm^{-1} , $\kappa = 1$ and $\Delta = 0$(high-symmetry case).

try limit ($\Delta = 0$) when the single ion anisotropy is excluded, whereas Figure 9 shows the barriers calculated in the limit of a strong negative axial field.

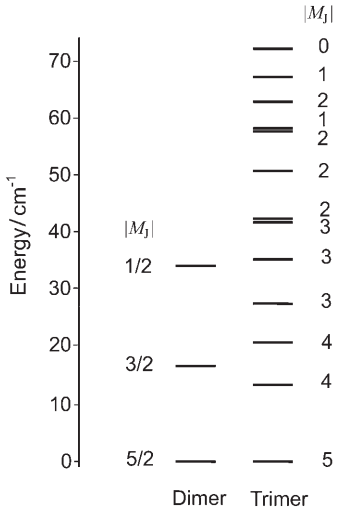

Figure 9. Comparison of the barriers for the reversal of magnetization for Mn(III)–Mn(II) (left) and Mn(II)–Mn(III)–Mn(II) (right) clusters calculated within the anisotropic exchange model with $J_{ex} = -4$ cm^{-1}, $\lambda = -180$ cm^{-1}, $\kappa = 1$ and $\Delta = -7000$ cm^{-1} (axial limit).

A large increase of the barrier for the trimer as compared to that for the dimer can be explained by the fact that the antiferromagnetic exchange between the central Mn(III) ion and the terminal Mn(II) ions couples two spins of the Mn(II) ions ($s_A = s_C = 5/2$) in parallel, thus strongly enhancing the total angular momentum of the entire system. This example clearly demonstrates that adding Mn ions to the finite alternating Mn(III)–Mn(II) linear chain is expected to lead to a strong increase in the barrier and hence to a significant enhancement in the observed SMM properties of the cyanide-based cluster.

The predicted possibility of raising the barrier U by increasing the number of metal ions in the linear cluster containing orbitally degenerate Mn(III) ions is expected to be practically achievable owing to the preference of cyanide moiety to adopt a linear bridging geometry between two metal centers.

8. Conclusions

The results obtained are summarized as follows:

1) The orbitally dependent superexchange between Mn(II) and Mn(III) ions in combination with the SO coupling acting within the ground $^3T_1$ term of the Mn(III) ion was found to create an appreciable barrier for the reversal of magnetization in dimeric Mn(III)–CN–Mn(II) clusters and linear trimeric Mn(II)–NC–Mn(III)–CN–Mn(II) clusters. The barrier significantly increases when passing from the dimer to the trimer, thus indicating the possibility of reaching higher blocking temperatures for SMMs by increasing the number of manganese ions in a finite linear alternating chain.
2) Along with the anisotropy caused by the orbitally dependent exchange, the negative axial crystal field acting on the Mn(III) ion may lead to a significant enhancement of the barrier. The combined effect of the local and exchange anisotropic terms on the barrier height significantly exceeds the sum of these two contributions considered separately. One can say that, providing $\Delta < 0$, the local and exchange contributions to the global magnetic anisotropy (and hence to the barrier) are mutually amplified.

The results obtained from this theoretical analysis are relevant to the issue of a more rational design approach for the synthesis of cyano-based SMMs with higher blocking temperatures. In forthcoming publications we plan to present synthetic aspects of this design and to demonstrate how the problem of the barrier increase can be solved with the aid of cyanide chemistry.

The theoretical approach presented here is based on the effective Hamiltonian with a set of semiempirical parameters. Remarkable progress in the understanding of the electronic structure of cyanide Mn(II)/Mn(III) compounds (mono- and dinuclear) has been made[27] with the aid of DFT calculations. A more complete description of the magnetic anisotropy can be made using a combined theory.

Acknowledgements

Financial support from the U.S. Civilian Research & Development Foundation for the Independent States of the Former Soviet Union (CRDF, award MOC2-2611-CH-04) and the Moldovan Research and Development Association (MRDA, award No. MTFP-04-07 under funding from CRDF) is appreciated. BST thanks the Council for Higher Education of Israel and VATAT for financial support. KRD gratefully acknowledges the Department of Energy (DOE-FG03-02ER45999).

Keywords: cluster compounds · cyano-bridged manganese clusters · exchange interactions · magnetic properties

[1] D. Gatteschi, R. Sessoli, *Angew. Chem.* **2003**, *115*, 278; *Angew. Chem. Int. Ed.* **2003**, *42*, 269.
[2] D. D. Awschalom, D. P. Di Vencenzo, *Phys. Today* **1995**, *48*, 43.
[3] R. Sessoli, H.-L. Tsai, A. R. Schake, S. Wang, J. B. Vincent, K. Folting, D. Gatteschi, G. Christou, D. N. Hendrickson, *J. Am. Chem. Soc.* **1993**, *115*, 1804.
[4] R. Sessoli, D. Gatteschi, A. Caneschi, M. A. Novak, *Nature* **1993**, *365*, 141.
[5] H. J. Eppley, H.-L. Tsai, N. de Vries, K. Folting, G. Christou, D. N. Hendrickson, *J. Am. Chem. Soc.* **1995**, *117*, 301.
[6] S. M. J. Aubin, Z. Sun, L. Pardi, J. Krzystek, K. Folting, L.-C. Brunel, A. L. Rheingold, G. Christou, D. N. Hendrickson, *Inorg. Chem.* **1999**, *38*, 5329.
[7] M. Soler, S. K. Chandra, D. Ruiz, E. R. Davidson, D. N. Hendrickson, G. Christou, *Chem. Commun.* **2000**, 2417.
[8] A. Müller, M. Luban, C. Schröder, R. Modler, P. Kögerler, M. Axenovich, J. Schnack, P. Canfield, S. Bud'ko, N. Harrison, *ChemPhysChem* **2001**, *2*, 517.
[9] A. J. Tasiopoulos, A. Vinslava, W. Wernsdorfer, K. A. Abboud, G. Christou, *Angew. Chem.* **2004**, *116*, 2169; *Angew. Chem. Int. Ed.* **2004**, *43*, 2117.
[10] J. J. Sokol, A. G. Hee, J. R. Long, *J. Am. Chem. Soc.* **2002**, *124*, 7656.
[11] H. J. Choi, J. J. Sokol, J. R. Long, *Inorg. Chem.* **2004**, *43*, 1606.
[12] C. P. Berlinguette, D. Vaughn, C. Cañada-Vilalta, J.-R. Galán-Mascarós, K. R. Dunbar, *Angew. Chem.* **2003**, *115*, 1561; *Angew. Chem. Int. Ed.* **2003**, *42*, 1523.
[13] S. Wang, J. L. Zuo, H. C. Zhou, H. J. Choi, Y. Ke, J. R. Long, *Angew. Chem.* **2004**, *116*, 6066; *Angew. Chem. Int. Ed.* **2004**, *43*, 5940.
[14] J. J. Borrás-Almenar, J. M. Clemente-Juan, E. Coronado, A. V. Palii, B. S. Tsukerblat, *J. Chem. Phys.* **2001**, *114*, 1148.
[15] J. J. Borrás-Almenar, J. M. Clemente-Juan, E. Coronado, A. V. Palii, B. S. Tsukerblat, *Chem. Phys.* **2001**, *274*, 131.
[16] J. J. Borrás-Almenar, J. M. Clemente-Juan, E. Coronado, A. V. Palii, B. S. Tsukerblat, *Chem. Phys.* **2001**, *274*, 145.
[17] A. V. Palii, B. S Tsukerblat, E. Coronado, J. M. Clemente-Juan, J. J. Borrás-Almenar, *J. Chem. Phys*, **2003**, *118*, 5566.
[18] V. S. Mironov, L. F. Chibotaru, A. Ceulemans, *J. Am. Chem. Soc.* **2003**, *125*, 9750.
[19] A. V. Palii, S. M. Ostrovsky, S. I. Klokishner, B. S. Tsukerblat, J. R. Galán-Mascarós, C. P. Berlinguette, K. R. Dunbar, *J. Am. Chem. Soc.* **2004**, *126*, 16860.
[20] B. S. Tsukerblat, A. V. Palii, S. M. Ostrovsky, S. V. Kunitsky, S. I. Klokishner, K. R. Dunbar, *J. Chem. Theory Comput.* **2005**, *1*, 668.
[21] P. W. Anderson, in *Magnetism* (Eds.: G. T. Rado, H. Suhl), Academic, New York, **1963**.
[22] S. Sugano, Y. Tanabe, H. Kamimura, *Multiplets of Transition-Metal Ions in Crystals*, Academic, New York London, **1970**.
[23] M. Nishino, Y. Yoshioka, K. Yamaguchi, *Chem. Phys. Lett.* **1998**, *297*, 51.
[24] H. Weihe, H. U. Güdel, *Comments Inorg. Chem.* **2000**, *22*, 75.
[25] J. B. Goodenough, *Magnetism and Chemical Bond*, Wiley Interscience, New York, **1963**.
[26] A. Abragam, B. Bleaney, *Electron Paramagnetic Resonance of Transition Ions*, Clarendon, Oxford, England, **1970**.
[27] C. Daul, C. Rauzi, S. decurtins, P. Franz, A. Hauser, *Int. J. Quantum Chem.* **2005**, *101*, 753.

Received: October 10, 2005

